High-Frequency Asymptotic Solution with Higher-Order Terms for Scattered Fields by an Impedance Discontinuity of a Planar Impedance Surface

[#]Toru Kawano, Keiji Goto, and Toyohiko Ishihara
Department of Communication Engineering, National Defense Academy
1-10-20 Hashirimizu, Yokosuka, Kanagawa 239-8686, Japan, E-mail: tkawano@nda.ac.jp

Abstract

The uniform asymptotic solution with higher-order terms for the scattered fields by the discontinuity of the impedance surface has been derived. The validity of the asymptotic solution has been confirmed by comparing with the reference solution calculated numerically. The physical interpretation of the asymptotic solution is also clarified.

Keywords : Planar impedance surface Asymptotic solution Higher-order terms

1. Introduction

Ground wave propagation along the earth's surface is strongly influenced by a discontinuity of the surface impedance of the earth [1] – [7]. It is assumed that both the transmitting and receiving antennas are placed on or near the earth's surface. The recovery effect [2] – [5] appearing on the portion of the sea over the land-to-sea mixed-path has been examined by using the mixed-path theory [2], [3]. The recovery effect has been confirmed experimentally through the measurement along the land-to-sea mixed-path [2], [3], [5] – [8].

In the present study, we shall examine the reflected and scattered fields when the source and observation points are placed sufficiently higher positions from the earth's surface [9] – [12]. The solution for the scattered fields by the discontinuity of the impedance surface has been derived by applying Wiener-Hopf technique [9], [10]. Here we shall derive a uniform asymptotic solution which contains the higher-order terms for the reflected and scattered fields by applying the aperture field method (AFM) to obtain the integral representation for the fields and the saddle point technique [13] to evaluate the integral asymptotically. Higher-order scattering terms are included in the high-frequency asymptotic solution [11] – [13].

We will confirm the validity and applicable range of the novel uniform asymptotic solution by comparing with the reference solution calculated numerically. The physical interpretation of the uniform asymptotic solution is also clarified in this paper.

2. Formulation and Higher-Order High-Frequency Asymptotic Solution

2.1 Formulation and Integral Representation

Figures 1(a) and 1(b) show the Cartesian coordinate system (x, y, z), a planar impedance surface with an impedance discontinuity, the junction C at $x = d$, transmitting and receiving antennas T and R, the geometrically reflected ray on the impedance surface, the scattered ray excited at the junction C, and the aperture plane defined by $x = d$, $-\infty < y < \infty$, $0 \le z < \infty$. The surface impedance changes at the junction x = C from Z_a $(=(\mu_0/\varepsilon_a^*)^{1/2}, \varepsilon_a^* = \varepsilon_a + i\sigma_a/\omega)$ to Z_b $(=(\mu_0/\varepsilon_b^*)^{1/2}, \varepsilon_b^* = \varepsilon_b + i\sigma_b/\omega)$. Here $(\varepsilon_a, \sigma_a)$ and $(\varepsilon_b, \sigma_b)$ denote (dielectric constant, conductivity) on the land and the sea, respectively. The vertical transmitting antenna is placed at T(0, 0, h) and the vertical receiving antenna is place at $R_2(x, 0, z)$ above the geometrical boundary (GB) or at $R_3(x, 0, z)$ below the GB as shown in Figs. 1(a) and 1(b), respectively. The geometrical ray reflected on the portion of the surface impedance Z_a (or Z_b) and the scattered ray diffracted by the junction at x = C are observed at the observation point $R_2(x, 0, z)$ (or $R_3(x, 0, z)$).

The vertical electric field E_z observed at the receiving antenna R_2 or R_3 due to the antenna current I and antenna height ℓ may be obtained from [6], [8], [11], [12]

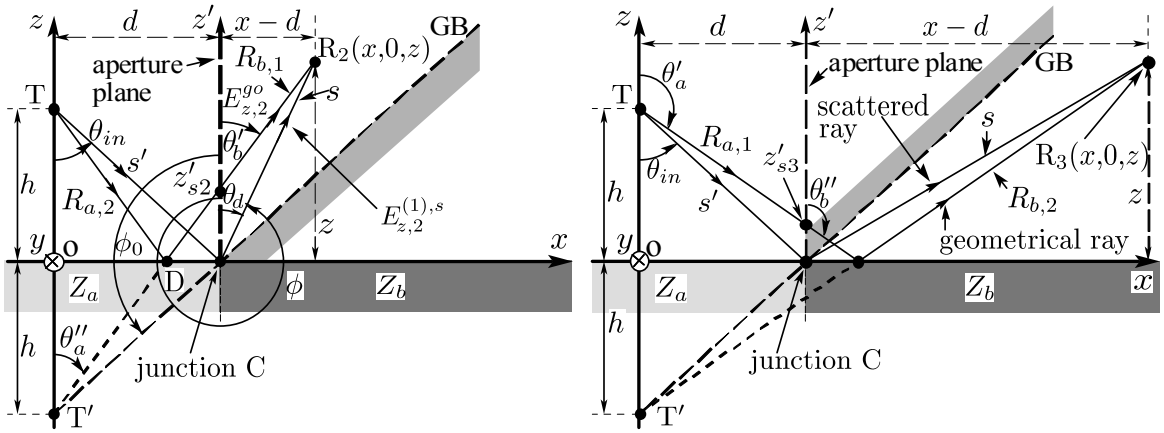

(a) Observation point R_2 placed above GB(geometrical boundary).

(b) Observation point R_3 placed below GB.

Figure 1: Cartesian coordinate system (x, y ,z), planar surface with impedance discontinuity at the junction x = C, and aperture plane.

$$E_z = \sum_{j=2}^{3} E_{z,j}, \quad E_{z,j} = -i\omega\mu_0 I\ell \frac{1}{4\pi}\sqrt{\frac{k_0}{2\pi}}e^{-i\frac{\pi}{4}}\int_0^\infty f_j(z')e^{ik_0 q_j(z')}dz', \quad j = 2 \text{ or } 3, \tag{1}$$

where the amplitude function $f_j(z')$ and the phase function $q_j(z')$ are given by

$$f_2(z') = \frac{\sin\theta''_a \sin\theta'_b \Gamma_a}{\sqrt{R_{a,2}R_{b,1}q_2(z')}}, \quad \Gamma_a = \frac{k_a(z'+h) - k_0 R_{a,2}}{k_a(z'+h) + k_0 R_{a,2}}, \quad q_2(z') = R_{a,2} + R_{b,1}, \tag{2a}$$

$$R_{a,2} = \sqrt{d^2 + (z'+h)^2}, \quad R_{b,1} = \sqrt{(x-d)^2 + (z-z')^2}, \tag{2b}$$

$$f_3(z') = \frac{\sin\theta'_a \sin\theta''_b \Gamma_b}{\sqrt{R_{a,1}R_{b,2}q_3(z')}}, \quad \Gamma_b = \frac{k_b(z+z') - k_0 R_{b,2}}{k_a(z+z') + k_0 R_{b,2}}, \quad q_3(z') = R_{a,1} + R_{b,2}, \tag{3a}$$

$$R_{a,1} = \sqrt{d^2 + (h-z')^2}, \quad R_{b,2} = \sqrt{(x-d)^2 + (z+z')^2}. \tag{3b}$$

In (1), z' is the integration variable on the aperture plane ($x = d$, $y = 0$, $0 \le z' < \infty$) and k_0 ($=\omega\sqrt{\varepsilon_0\mu_0}$), k_a ($=\omega\sqrt{\varepsilon_a^*\mu_0}$),and k_b ($=\omega\sqrt{\varepsilon_b^*\mu_0}$) denote respectively the wavenumbers in the air, on the surface with the surface impedance Z_a, and on the surface with the surface impedance Z_b. The notations θ'_a , θ''_a , θ'_b , θ''_b , $R_{a,1}$, $R_{a,2}$, $R_{b,1}$, and $R_{b,2}$ used in the above equations are defined in Figs. 1(a) and 1(b). The time factor $\exp(-i\omega t)$ is suppressed throughout this paper.

2.2 **Higher-Order High-Frequency Asymptotic Solution**

Since the asymptotic analysis method for the vertical electric field $E_{z,3}$ with j = 3 has been considered elsewhere [14], here we will investigate the analysis method for $E_{z,j}$ with j = 2. The physical interpretation of the index j (= 2 or 3) has been explained in [12].

When the observation point $R_2(x, 0, z)$ is placed near the GB (geometrical boundary) line, the saddle point $z' = z'_{s2}$ is located near the endpoint $z' = 0$ of the integral in (1). Therefore, by applying the saddle point technique applicable uniformly as the saddle point approaches the endpoint $z' = 0$ [11], [12], [14], one may derive the uniform asymptotic solution for the integral (1). Thus, the vertical electric field $E_{z,2}$ may be given by

$$E_{z,2} = E_{z,2}^{go} + E_{z,2}^{(1),s} + E_{z,2}^{(2),s} + E_{z,2}^{(3),s}, \tag{4}$$

$$E_{z,2}^{go} = -i\omega\mu_0 I\ell \frac{\exp\{ik_0(R_{a,2}+R_{b,1})\}}{4\pi(R_{a,2}+R_{b,1})}\Gamma_a \sin^2\theta''_a, \quad E_{z,2}^{(1),s} = E_{in}^r D_2^{(1)} E_{z,d}. \tag{5}$$

In (4) and (5), $E_{z,2}^{go}$ and $E_{z,2}^{(1),s}$ denote, respectively, the geometrical ray $T \to D \to R_2$ reflected on the surface with the impedance Z_a (see Fig. 1(a)) and the scattered ray $T \to C \to R_2$ diffracted by the discontinuity of the surface impedance at the junction x = C. The terms E_{in}^r, $D_2^{(1)}$, and $E_{z,d}$

constituting the scattered ray solution $E_{z,2}^{(1),s}$ are given by

$$E_{in}^{r} = -i\omega\mu_0 I\ell \frac{\exp(ik_0 s')}{4\pi s'} \sin\theta_{in}, \quad D_2^{(1)} = \frac{\exp(i\pi/4)}{2\sqrt{2\pi k_0}} \tan\frac{\phi-\phi_0}{2} F(X^{GB})\Gamma_a, \tag{6}$$

$$F(X) = -2i\sqrt{X}e^{-iX}\int_{\sqrt{X}}^{\infty} e^{i\tau^2} d\tau, \quad X^{GB} = 2k_0 \frac{s's}{s'+s}\cos^2\frac{\phi-\phi_0}{2}, \tag{6a}$$

$$E_{z,d} = \sqrt{\frac{s'}{s(s'+s)}}\, e^{ik_0 s} \sin\theta_d, \tag{7}$$

where E_{in}^{r} and $E_{z,d}$ denote, respectively, the incident ray on the junction x = C and the scattered ray propagating from C to the observation point R_2 in Fig. 1(a). While, $E_{z,2}^{(2),s}$ in (4) corresponding to the second-order asymptotic solution for the scattered ray $T \to C \to R_2$ may be given by

$$E_{z,2}^{(2),s} = E_{in}^{r} D_2^{(2)} E_{z,d}, \quad D_2^{(2)} = \frac{\exp(i\pi/4)}{\sqrt{2\pi k_0}} \Gamma_a' \frac{s'^2 s}{d(s'+s)}, \quad \Gamma_a' = \frac{2k_a k_0 (s'^2 - h^2)}{s'(k_a h + k_0 s')^2}. \tag{8}$$

The last term $E_{z,2}^{(3),s}$ in (4) represents the scattered ray ($T \to C \to R_2$) solution higher than and equal to the third-order asymptotic approximation. The novel higher-order asymptotic solution may be given by

$$E_{z,2}^{(3),s} = E_{z,2}^{(3),s,1} + E_{z,2}^{(3),s,2} + E_{z,2}^{(3),s,3}, \tag{9}$$

$$E_{z,2}^{(3),s,1} = \frac{A_2(0)}{2k_0} \cdot \frac{s'(s'+s)}{\sqrt{2}d\,\Gamma_a} e^{-i\pi/4}\left(1+\gamma(k_0)\right) E_{z,2}^{(1),s}, \quad \gamma(k_0) = \frac{E_{z,2}^{go}}{E_{z,2}^{(1),s}} \tag{10}$$

$$E_{z,2}^{(3),s,2} = \frac{1}{2k_0} \cdot \frac{A_2(S_{2a}) - A_2(0)}{S_{2a}} \cdot \frac{(s'+s)^{3/2}}{2i(s's)^{1/2}\Gamma_a'} E_{z,2}^{(2),s}, \tag{11}$$

$$E_{z,2}^{(3),s,3} = \frac{-i\omega\mu_0 I\ell}{(2k_0)^2} \cdot \frac{1}{4\pi}\sqrt{\frac{k_0}{2\pi}} e^{-i\frac{\pi}{4}} e^{ik_0 q_2(z'_{2s})} I_2^{(3)}, \; I_2^{(3)} = \int_{S_{2a}}^{\infty} \frac{d}{ds}\frac{A_2(s) - A_2(0)}{s} e^{-k_0 s^2} ds, \tag{12}$$

where, $E_{z,2}^{(3),s,1}$ and $E_{z,2}^{(3),s,2}$ in (10) and (11) denote, respectively, the third-order and the fourth-order asymptotic solutions for the scattered ray $T \to C \to R_2$. The last term $E_{z,2}^{(3),s,3}$ in (9), which is defined by (12) corresponds to the scattered ray solution higher than and equal to the fifth-order asymptotic solution. This term may be neglected in the high-frequency condition where $k_0 >> 1$. The notations used in the above equations are defined as follows [14]

$$A_2(s) = \frac{G_2(s) - G_2(0)}{s}, \quad G_2(s) = f_2(z')\frac{dz'}{ds}, \tag{13}$$

$$iq_2(z') = iq_2(z'_{2s}) - s^2, \quad S_{2a} = \sqrt{i\{q_2(z'_{2s}) - q_2(0)\}}. \tag{14}$$

The notation z'_{s2} denotes the saddle point of the integrand in (1) in the complex z' - plane.

So far, we have derived the uniform asymptotic solution for $E_{z,2}$ defined in (1). As shown in (1), in order to obtain the total field at R_2 (see Fig. 1(a)), it is necessary to add the asymptotic solution for $E_{z,3}$ defined in (1) to $E_{z,2}$ in (4). The asymptotic solution for $E_{z,3}$ may be found elsewhere [14], [15].

3. Numerical Results and Discussions

In Figs. 2(a) and 2(b), we have compared the calculation results obtained from the uniform asymptotic solution proposed in this study with the reference solution calculated from (1) by performing the numerical integration. Vertical electric field magnitudes are calculated as the function of the distance x (λ). In both Figs. 2(a) and 2(b), it is observed that the uniform asymptotic solution including fourth-order asymptotic solution (○ ○ ○ : open circles) agrees very well with the reference solution (—— : solid curves) in the whole region shown in the figures. However, when the observation point is placed at the lower position as in Fig. 2(a), the first-order asymptotic solution (– – –) and the second-order asymptotic solution (— · —) deviate from the reference solution (——) in the ranges x > 750λ. The errors of these asymptotic solutions are relatively large as shown

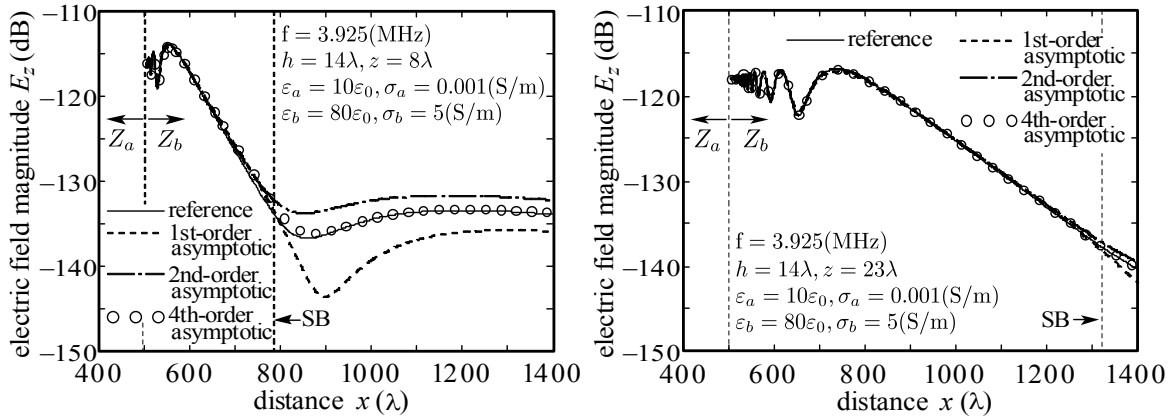

(a) Observation point is located at lower position.

(b) Observation point is located at sufficiently higher position.

Figure 2: Comparisons of uniform asymptotic solutions with the reference solution.

in Fig. 2(a). However, if we increase the height of the receiving antenna, the first-order and second-order asymptotic solutions agree very well with the reference solution up to $x = 1350\lambda$ as shown in Fig. 2(b).

4. Conclusion

By applying the aperture field method and the saddle point technique applicable uniformly as the saddle point approaches the endpoint of the integration path, we have derived the higher-order asymptotic solution for the scattered fields by the discontinuity of the planar impedance surface. We have confirmed the validity and importance of the higher-order asymptotic solution by comparing with the reference solution. Also shown is the physical interpretation of the asymptotic solution for the scattered fields.

References

[1] K. Furutsu, Journal of the Radio Research Laboratories, vol.2, no.10, pp.345-398, Oct. 1955.
[2] J. R. Wait, Journal of Research of the National Bureau of Standards, vol.57, no.1, pp.1-15, July 1956.
[3] J. R. Wait, IEEE Antennas and Propagation Magazine, vol.40, no.5, pp.7-24, Oct. 1998.
[4] L. Sevgi and L. B. Felsen, Int. Journal of Numer. Model. : Electronic Networks, Devices and Fields, vol.11, pp.87-103, Nov. 1998.
[5] T. Kawano, K. Goto, and T. Ishihara, IEICE Trans. on Electron., vol.E90-C, no.2, pp.288-294, Feb. 2007.
[6] T. Kawano, K. Goto, and T. Ishihara, IEICE Trans. on Electron., vol.E92-C, no.1, pp.46-54, Jan. 2009.
[7] T. Kawano, K. Goto, and T. Ishihara, IEICE Trans. on Electron., vol.E94-C, no.1, pp.10-17, Jan. 2011.
[8] T. Kawano, K. Goto, and T. Ishihara, IEEE AP-S Int. Symp., Charleston, CD-ROM (ISBN:978-1-4244-3647-7), June 2009.
[9] R. G. Rojas, IEEE Trans. on Antennas and Propag., vol.36, no.1, pp.71-83, Jan. 1988.
[10] T. Lertwiriyaprapa, P. H. Pathak, and J. L. Volakis, Radio Science, vol.42, RS6S18, doi:10.1029/2007RS003689, 2007.
[11] T. Kawano, K. Goto, and T. Ishihara, IEEE AP-S Int. Symp., Tronto, CD-ROM (ISBN: 978-1-4244-4968-2), July 2010.
[12] T. Kawano, K. Goto, and T. Ishihara, IEICE Electronics Express, vol.7, no.14, pp.1072-1078, July 2010.
[13] L. B. Felsen and N. Marcuvitz eds., Radiation and Scattering of Waves, chap.4, IEEE Press, (Classic Reissue), New Jersey, 1994.
[14] T. Kawano, K. Goto, and T. Ishihara, IEEE AP-S Int. Symp., Spokane, July 2011 (to be appeared).
[15] T. Kawano, K. Goto, and T. Ishihara, The Papers of Technical Meeting on Electromagnetic Theory, IEE Japan, EMT-10-90, pp.159-164, July 2010.

Acknowledgments

This work was supported in part by the Grant-in-Aid for Scientific Research (C) (21560424) from Japan Society for the Promotion of Science (JSPS).